HEAT TRANSFER-ASIAN RESEARCH (WILEY)

Accepted November 30th 2019

DIFFERENTIAL TRANSFORM SOLUTION FOR HALL AND ION SLIP EFFECTS ON RADIATIVE-CONVECTIVE CASSON FLOW FROM A STRETCHING SHEET WITH CONVECTIVE HEATING

M. M. Bhatti[1,2*], S. U. Khan[1], O. Anwar Bég[3] and **A. Kadir[3]**

[1]*College of Mathematics and Systems Science, Shandong University of Science and Technology, Qingdao, Shandong, 266590,* ***China.***

[2]*Shanghai Institute of Applied Mathematics and Mechanics, Shanghai University, Shanghai 200072,* ***China.***

[3]*Department of Mechanical/Aeronautical Engineering, Salford University, Manchester, M54WT,* ***UK.***

***Corresponding author :** muhammad09@shu.edu.cn; mmbhatti@sdust.edu.cn*

ABSTRACT:

Magnetohydrodynamic (MHD) materials processing is becoming increasingly popular in the 21st century since it offers significant advantages over conventional systems including improved manipulation of working fluids, reduction in wear and enhanced sustainability. Motivated by these developments, the present work develops a mathematical model for Hall and Ion slip effects on non-Newtonian Casson fluid dynamics and heat transfer towards a stretching sheet with a convective heating boundary condition under a transverse magnetic field. The governing conservation equations for mass, linear momentum and thermal (energy) are simplified with the aid of similarity variables and Ohm's law. The emerging nonlinear coupled ordinary differential equations are solved with an analytical technique known as the differential transform method (DTM). The impact of different emerging parameters is presented and discussed with the help of graphs and tables. Generally aqueous electro-conductive polymers are considered for which a Prandtl number of 6.2 is employed. With increasing Hall parameter and ion slip parameter the flow is accelerated whereas it is decelerated with greater magnetic parameter and rheological (Casson) fluid parameter. Skin friction is also decreased with greater magnetic field effect whereas it is increased with stronger Hall parameter and ion slip parameter values.

KEYWORDS: *Hall current; ion slip; thermal slip; heat transfer; electro-conductive polymer processing; differential transform method (DTM).*

NOMENCLATURE

$\tilde{u}, \tilde{v}$	Velocity components
x, y	Cartesian coordinates
$\tilde{p}$	Pressure
Re	Reynolds number
$\tilde{t}$	Time
P_r	Prandtl number
$\bar{k}$	Mean absorption coefficient

B_i	Biot number
J	Current density
$\tilde{T}_w$	Sheet temperature
$\tilde{T}_\infty$	Free stream temperature
M	Hartmann (magnetic) number
B	Magnetic field
R_d	Radiation parameter

GREEK SYMBOLS

$\bar{\alpha}$	Thermal conductivity
τ	Stress tensor
β	Casson viscoplastic fluid parameter
ω_e	Cyclotron frequency
τ_e	Electron collision time
β_i	Ion slip parameter
β_e	Hall parameter
$\bar{\sigma}$	Stefan-Boltzmann constant
μ	Dynamic viscosity of the Casson fluid
θ	Temperature profile
σ	Electrical conductivity
φ	Stream function
c_p	Specific heat
ν	Kinematic viscosity of the Casson fluid

1.INTRODUCTION

Industrial materials fabrication frequently features non-Newtonian fluid flows from a heated surface which may be stretched or contracted [1]. Examples include plastic sheet synthesis, polymer extrusion, food stuff manufacturing (chocolate, toffee etc), floating glass production, biopolymer packaging rolls, spray coating etc. In many applications a convectively heated surface

is used and special thermal boundary conditions must be employed in mathematical models [2,3]. Additionally, the constitution of manufactured materials is strongly influenced by skin friction, stretching rates of the sheet and the rate of heat transfer to the sheet. Various authors have therefore investigated the *non-Newtonian fluid flow with heat transfer from stretching surfaces*. The associated boundary value problems have also been studied with diverse numerical and analytical methods. Hayat and Sajid [4] investigated analytically and numerically the heat transfer with the axisymmetric flow of second-grade fluid through a stretching sheet. They discussed two cases, namely the prescribed surface heat flux and prescribed surface temperature scenario. Nadeem *et al.* [5] examined the non-orthogonal stagnation point flow with heat transfer of a second grade viscoelastic nanofluid towards a stretching sheet. Latiff *et al.* [6] used MAPLE shooting quadrature to study the time-dependent bioconvection micropolar slip flow, heat and mass diffusion from expanding/contracting sheets. Hayat *et al.* [7] presented homotopy analysis method (HAM) solutions for transient stretching sheet flow, heat and mass transfer in a chemically reactive third-grade viscoelastic fluid (HAM). Bég *et al.* [8] used an electrothermal network simulation code to study the time-dependent natural convection boundary layer flow from a stretching sheet in a Darcy-Forchheimer medium saturated with Walters-B elastico-viscous liquid. These studies all confirmed the significant modification in transport phenomena induced by rheological behavior.

Heat transfer under the influence of magnetic field is also an important area of modern technology and features in "green" energy systems, blood flow control, liquid metal processing, nuclear energy plasma control, electromagnetic casting and also electro-conductive (magnetic) materials synthesis. Magnetic polymers are a special sub-branch of magnetic materials which combine the electrical conductivity features of metals with the non-Newtonian and adaptive characteristics of polymers [9]. Such materials provide a new level of sophistication for smart coating systems [10, 11]. To simulate the manufacture of these fluids, mathematical models must combine magnetohydrodynamics (MHD) and rheology and often powerful numerical techniques are required to solve the resulting conservation equations. The use of these advanced multi-physical fluid dynamics models can significantly improve fabrication processes for such materials and leads to an optimization of quality control, in particular, for heat and mass transfer. With judicious use of an applied magnetic field the polymer constitution and performance can be manipulated and furthermore flow instabilities may be suppressed and homogeneity sustained in products. Many investigators have simulated magnetic polymer flows with heat and mass diffusion

in stretching sheet (extrusion) flows. Gupta *et al.* [12] used a variational finite element code to analyze the magnetic micropolar stretching sheet thermal convection flow in the vicinity of a stagnation point. Kumar *et al.* [13] used MATLAB routines to simulate transient magnetic non-Newtonian nanofluid convective heat transfer from an extending sheet with Joule heating and Stokes couple stress rheological model. Vasu *et al.* [14] used homotopy and generalized differential quadrature methods to study magnetized bioconvection of a viscoplastic (Casson) fluid from a stretching surface. Prasad *et al.* [15] used Runge-Kutta quadrature to compute the influence of variable viscosity on magnetized viscoelastic fluid flow with heat transfer from a stretching surface, noting that the skin friction coefficient decreases due to the increment in a magnetic field.

In high-temperature fabrication of polymers [16], *radiative heat transfer* arises in addition to thermal conduction and thermal convection. To simulate radiative flux often an *algebraic flux approximation* is popular and some examples include the Rosseland diffusion model, Hamaker six flux model, Milne-Eddington model, Schuster-Schwartzchild model and Traugott P1 flux model. In multi-physical coating flows, the Rosseland model has been shown to be reasonably accurate for high optical thicknesses. Although it does not allow optical thickness or spectral effects to be simulated, it does provide a mechanism for evaluating the relative role of thermal conduction and thermal radiation flux. Radiative heat transfer using the Rosseland model in transport from stretching surfaces has therefore received considerable attention for both Newtonian and non-Newtonian fluids and also magnetic and non-magnetic scenarios. Uddin *et al.* [17] studied radiative heat flux impact on nanofluid stretching sheet flow with a Buongiorno nanoscale model. Combined magnetohydrodynamic and radiative effects were considered by Abo-Eldahab and El Gendy [18] for variable viscosity flow towards a stretching sheet. Hayat *et al.* [19] studied variable thermal conductivity and thermal radiation effects on Jeffrey viscoelastic three-dimensional stretching sheet flow. Hayat *et al.* [20] considered the influence of Joule heating and thermal radiation of third-grade fluid from an extending surface. Bhatti *et al.* [21] used a successive linearization method to study the impact of thermal relaxation and thermal radiation on magnetic polymer stretching flow with a Maxwell viscoelastic model. Further studies have used the Carreau rheological model [22] and the Williamson model [23].

In magnetohydrodynamic materials processing, in addition to the customary transverse static magnetic field which induces a Lorentzian retarding force, multiple other phenomena can arise. These include alternating magnetic fields, Alfven waves, magnetic leakage, magnetic

induction, magnetic dipoles, Hall currents and ion slip currents [24]. Under stronger magnetic fields both Hall and ion slip currents may become significant. The former relates to a secondary (cross) flow being induced in the regime and also decreases medium electrical conductivity. The latter concerns the presence of partial ionization in liquids (or gases) and reduces the electrical conductivity of the fluid. Both Hall and ionslip currents have been studied by several researchers in the context of engineering MHD flows and observed to influence the magnitude and direction of the current density and consequently the impact of the magnetic body force. Bég *et al.* [25] studied oblique magnetic field and Hall current effects on rotating MHD flow in a channel containing a porous medium. Pal *et al*. [26] presented perturbation solutions for the impact of Hall current and thermal radiation on oscillatory mixed convection flow of a rotating micropolar. Ramesh *et al.* [27] studied the influence of hydrodynamic slip and Hall currents on non-Newtonian dusty fluid peristaltic pumping in a magnetic field. Attia *et al.* [28] presented power series solutions for transient two-phase hydromagnetic viscous flow in a pipe with Hall and ion slip effects. In the area of stretching sheet flows, Shateyi and Motsa [29] employed a Chebyshev pseudo-spectral collocation scheme to compute the boundary layer flow, heat and mass transfer in transient magnetohydrodynamic flow from a stretching sheet. Ion slip effects on non-Newtonian magnetic convection flow were examined by Choudhury and Dar [30] who noted the significant modification in velocity field with stronger ion slip. Further studies of Hall current and ionslip in magnetohydrodynamics have been communicated by Zueco *et al.* [31] for isothermal channels and Bég *et al.* [32] for non-isothermal stretching flow with Ohmic heating.

A close inspection of the literature indicates that thus far the combined impact of *Hall and ion slip effects with heat transfer on magnetohydrodynamic Casson fluid flow from a stretching surface with thermal slip and thermal radiation*, has not been considered. The governing flow problem is modeled with the help of Ohms law, mass, momentum and thermal energy conservation equations. The transformed ordinary differential equation boundary value problem is solved analytically with the Differential transform method (DTM). Validation with numerical quadrature (ND Solve routine in MATHEMATICA symbolic software) is included. The impact of selected magnetic, thermal and non-Newtonian parameters on velocity, temperature, skin friction and heat transfer- rates is visualized graphically and interpreted at length. The simulations are relevant to magnetic polymer processing technologies [33]. This paper is organized as follows: Sec. (1) presents a detailed introduction and problem justification. Sec. (2) deals with the mathematical

formulation of the problem. Sec. (3) describes the solution methodology. Sec. (4) is devoted to graphical and numerical results.

2.MATHEMATICAL FORMULATION

Let us consider the magnetohydrodynamic (MHD) viscous, incompressible, steady-state boundary layer flow and thermal convection heat transfer in an electro-conductive polymer from a stretching sheet at the stagnation point $y = 0$. The Casson (viscoplastic) fluid model is utilized. An external magnetic field B_0 is applied while the induced magnetic field is ignored due to small magnetic Reynolds number. Electron pressure is negligible. Magnetic field is sufficiently strong to generate a Hall current which gives rise to a secondary (cross flow) and also mobilize ion slip. A Cartesian coordinate system is adopted in which x −axis is taken along the direction of the sheet and y −axis is considered normal to it as shown in **Fig. 1**. $\tilde{T}_w$ denotes the temperature at the sheet and the temperature in the free stream is $\tilde{T}_\infty$. The polymer is assumed to be optically dense and a radiative flux is applied transverse to the sheet.

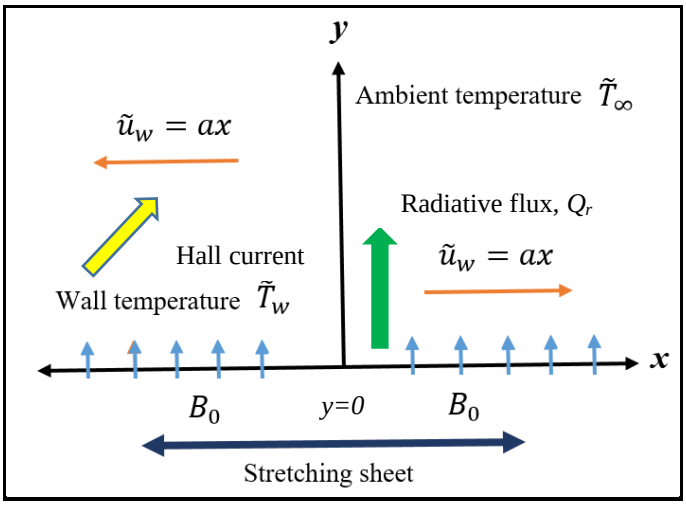

Figure 1. Physical model for magnetic non-Newtonian stretching flow.

The rheological equation of state for an isotropic and incompressible Casson (viscoplastic) fluid [34-36] is:

$$\boldsymbol{r_{ij}} = \begin{cases} \mathbf{2}\varepsilon_{ij}\left(\boldsymbol{\mu_b} + \dfrac{\boldsymbol{p_y}}{\sqrt{\mathbf{2\Pi}}}\right), \mathbf{\Pi_c < \Pi}, \\ \mathbf{2}\varepsilon_{ij}\left(\boldsymbol{\mu_b} + \dfrac{\boldsymbol{p_y}}{\sqrt{\mathbf{2\Pi_c}}}\right), \mathbf{\Pi_c > \Pi}, \end{cases} \tag{1}$$

where $\mathcal{E}_{ij}$ is the component of the deformation rate, Π is the product of the deformation rate and Π_c is the critical value of the plastic dynamic viscosity. The governing boundary layer equations for the regime can be written as [34]

$$\frac{\partial \tilde{u}}{\partial x} + \frac{\partial \tilde{v}}{\partial y} = 0, \tag{2}$$

$$\tilde{u}\frac{\partial \tilde{u}}{\partial x} + \tilde{v}\frac{\partial \tilde{v}}{\partial y} = \nu\left(1 + \frac{1}{\beta}\right)\frac{\partial^2 \tilde{u}}{\partial y^2} + \mathbf{J} \times \mathbf{B}, \tag{3}$$

$$\tilde{u}\frac{\partial \tilde{T}}{\partial x} + \tilde{v}\frac{\partial \tilde{T}}{\partial y} = \bar{\alpha}\frac{\partial^2 \tilde{T}}{\partial y^2} - \frac{1}{\rho c_p}\frac{\partial Q_r}{\partial y}, \tag{4}$$

The nonlinear radiative heat flux can be written following the Rosseland diffusion approximation as follows [18-23]:

$$Q_r = -\frac{16\bar{\sigma}\tilde{T}^3}{3\bar{k}}\frac{\partial \tilde{T}}{\partial y}. \tag{5}$$

The generalized form of Ohm's law with Hall and ion-slip effect can be written as:

$$\mathbf{J} = \sigma(\mathbf{E} + \mathbf{V} \times \mathbf{B}) - \frac{\omega_e \tau_e}{\mathbf{B}}(\mathbf{J} \times \mathbf{B}) - \frac{\omega_e \tau_e \beta_i}{\mathbf{B^2}}[(\mathbf{J} \times \mathbf{B}) \times \mathbf{B}]. \tag{6}$$

where $\beta_e = \omega_e \tau_e$ is the Hall parameter. The wall and free stream boundary conditions are imposed as:

$$\tilde{u} = ax, -k\frac{\partial \tilde{T}}{\partial y} = h\left(\tilde{T}_w - \tilde{T}\right), \text{at } y = 0, \tag{7}$$

$$\tilde{u} \to 0, \tilde{v} \to 0, \tilde{T} \to \tilde{T}_\infty \text{ at } y \to \infty. \tag{8}$$

The stream function (φ) can be defined as:

$$\tilde{u} = \frac{\partial \varphi}{\partial y}, \tilde{v} = -\frac{\partial \varphi}{\partial x}. \tag{9}$$

Introducing the following similarity transformation variables:

$$\zeta = \sqrt{\frac{a}{\nu}}y, R_d = \frac{4\bar{\sigma}\tilde{T}^3}{\rho c_p \bar{k}}, \tilde{u} = axf', M^2 = \frac{B_0^2\sigma}{c\rho}, \tilde{v} = -\sqrt{a\nu}f,\ \theta = \frac{\tilde{T}-\tilde{T}_\infty}{\tilde{T}_w-\tilde{T}_\infty}, P_r = \frac{\nu}{\bar{\alpha}}, B_i = \frac{h}{k}\sqrt{\frac{\nu}{a}}, \bar{\alpha} = \frac{k}{\rho c_p}. \tag{10}$$

and using Eqn. (8) in to Eq. (1) to Eq. (7), leads to:

$$\left(1+\frac{1}{\beta}\right)f''' - f'^2 + ff'' - \frac{M^2(1+\beta_i\beta_e)}{(1+\beta_e\beta_i)^2+\beta_e^2}f' = 0, \tag{11}$$

$$\left(\frac{1}{P_r}+\frac{4}{3}R_d\right)\theta'' + f\theta' = 2\theta f'. \tag{12}$$

Their corresponding boundary conditions are:

$$f(0) = 0, f'(0) = 1, f'(\infty) \to 1, \tag{13}$$

$$\theta'(0) = B_i(\theta(0)-1), \theta(\infty) \to 0. \tag{14}$$

Here all parameters have been defined in the notation. It is worth mentioning that the above results can be reduced to Newtonian fluid by taking $\beta \to \infty$ as a special case of our study. The physical quantities of interest for the governing flow problem are *skin friction coefficient* and *local Nusselt number* which in dimensionless form are defined as [34]:

$$C_F = C_f \mathrm{Re}_x^{1/2} = \left(1+\frac{1}{\beta}\right)f''(0), Nu_r = \frac{Nu_x}{\mathrm{Re}_x^{1/2}} = -\left(1+\frac{4}{3}R_d\right)\theta'(0), \tag{15}$$

where C_F and Nu_r are the dimensionless skin friction coefficient and Nusselt number, respectively whereas $\mathrm{Re}_x = \tilde{u}_w x/\nu$ is the local Reynolds number.

3. DIFFERENTIAL TRANSFORM SOLUTIONS

To solve the derived coupled nonlinear ordinary differential equations (11) and (12) under boundary conditions (13) and (14), a numerical or semi-analytical/numerical scheme is required. Many such techniques are available including the variational iteration method (VIM), homotopy analysis method (HAM), generalized differential quadrature (GDQ) etc. The differential transform method (DTM) method introduced by Zhou [37] is an alternative approach and is a very powerful technique for nonlinear problems. It has been employed in recent years to simulate a variety of viscous flow problems including peristaltic viscoelastic pumping [38], swirling Von Karman

hydromagnetic flow [39], polymer sheet stretching [40] and viscous hypersonic aerodynamics [41]. The transformation for the n^{th} derivative of a function in a single variable can be described as

$$\mathbb{F}(n) = \frac{1}{n!}\left(\frac{d^n \mathbb{f}}{d\xi^n}\right)_{\xi=\xi_0}, \tag{16}$$

where $\mathbb{f}(\boldsymbol{\xi})$ is the original function and $\mathbb{F}(\boldsymbol{n})$ is the transformed function and its inverse function can be defined as:

$$\mathbb{f}(n) = \sum_{n=0}^{\infty} \mathbb{F}(n)(\xi - \xi_0)^n. \tag{17}$$

The basics theme of the differential transform method is obtained using Taylor series expansion and in real applications, the function $\mathbb{f}(\boldsymbol{n})$ is defined by finite series which maybe expressed as follows:

$$\mathbb{f}(n) \cong \sum_{n=0}^{M} \mathbb{F}(n)(\xi - \xi_0)^n. \tag{18}$$

The value of $\boldsymbol{M}$ depends upon the convergence of the series. Now applying DTM to Eqns. (11)-(14), we have:

$$\mathbb{f}[n+3] = \sum_{r=0}^{n} \frac{-\mathbb{f}[n]\mathbb{f}[n-r+2](n-r+1)(n-r+2)}{\left(1+\frac{1}{\beta}\right)(n+1)(n+2)(n+3)} + \sum_{r=0}^{n} \frac{\mathbb{f}[r+1]\mathbb{f}[n-r+1](r+1)(n-r+1)}{\left(1+\frac{1}{\beta}\right)(n+1)(n+2)(n+3)} + \frac{(n+1)\mathbb{f}[n+1]}{\left(1+\frac{1}{\beta}\right)(n+1)(n+2)(n+3)} \frac{M^2(1+\beta_i\beta_e)}{(1+\beta_e\beta_i)^2+\beta_e^2}. \tag{19}$$

$$\mathbb{g}[n+2] = \frac{2\mathbb{g}[n](n+1)\mathbb{f}[n+1] - \mathbb{f}[n](n+1)\mathbb{g}[n+1]}{(n+1)(n+2)\left(\frac{1}{Pr}+\frac{4}{3}R_d\right)}. \tag{20}$$

The appropriate form of the boundary conditions is:

$$\mathbb{f}[0] = 0, \mathbb{f}[1] = 1, \mathbb{f}[2] = \frac{\alpha}{2}, \mathbb{g}[1] = -B_i(1 - \mathbb{g}[0]), \mathbb{g}[1] = \gamma. \tag{21}$$

Here $\boldsymbol{\alpha}$ and $\boldsymbol{\gamma}$ are constants. To validate the DTM solutions the entire boundary value problem has also been solved with the ND Solve routine in Mathematica software. This employs a shooting technique. The comparison of Differential Transform Method (DTM) and ND Solve solutions is

given in Table 1 for skin friction coefficient and Nusselt number. Generally, very close correlation is achieved and confidence in the DTM solutions is therefore justifiably high. In these solutions radiative heat transfer, magnetic body force, Hall and ionslip current effects are all present. Aqueous electro-conductive polymers are considered for which a Prandtl number of 6.2 is employed. With increasing Hall parameter and ion slip parameter the skin friction is increased i.e. the flow is accelerated whereas it is decelerated with greater magnetic parameter. Average Nusselt numbers are elevated with increasing Prandtl number and also with increasing radiative parameter. **Table 2** further shows the numerical comparison between the present DTM results and the previously published results of Gorla and Sidawi [43] ($\beta \to \infty, M = 0$ i.e. Newtonian, non-magnetic) and Abolbashari *et al*. [**34**] ($M = 0$ i.e. non-magnetic), and close correlation is achieved in both cases. Confidence in the DTM solutions is therefore justifiably high.

Table 1: Comparison between numerical and analytical results for skin friction coefficient (C_F) and Nusselt number (Nu_r) for various values of P_r, R_d, M, β_e and β_i

M	β_e	β_i	P_r	R_d	C_F (DTM)	C_F (NDSolve)	Nu_r(DTM)	Nu_r(NDSolve)
1	0.2	0.2	6.2	0.2	−1.7460	−1.7460		
2					−2.4820	−2.4820		
3					−3.3704	−3.3704		
	0.5				−1.6472	−1.6472		
	1				−1.5585	−1.5585		
	1.5				−1.5145	−1.5145		
		0.6			−1.6419	−1.6419		
		1.2			−1.5637	−1.5637		
		1.6			−1.5345	−1.5345		
			3				0.4977	0.4977
			4				0.5065	0.5065
			10				0.5246	0.5246
				0.5			0.6278	0.6278
				0.8			0.7316	0.7316
				1			0.7969	0.7969

Table 2: Comparison between present results and previously published results for $f''(0)$.

	Gorla and Sidawi [43]	Abolbashari *et al.* [34]
	$\beta \to \infty, M = 0$	$M = 0$
	-1.01435	-0.74127
Present results	-1.01435	-0.74127

4.NUMERICAL RESULTS AND DISCUSSION

This section elucidates the graphical results and discussion for the influence on velocity and temperature distributions with the different physical parameters arising in the governing flow problem i.e. Hartmann number M, Hall parameter β_e, Ion slip parameter β_i, Biot number B_i, rheological (Casson) fluid parameter β, Prandtl number P_r and radiation parameter R_d, respectively. For this purpose, Fig. (2) to Fig. (8) are sketched. As noted earlier, the case for a Newtonian fluid can be retrieved by taking $\beta \to \infty$. Moreover, the presents results can be reduced to the results obtained by Abolbashari *et al.* [27] by taking $M = \beta_i = \beta_e = 0$ i.e. non-magnetic case neglecting Hall and ion slip effects. It is further of note that $P_r = 6.2$ is prescribed. The polymers considered are *aqueous-based* so that the dominant thermophysical properties are water-controlled. They still feature rheological viscoplastic features but the Prandtl number is approximately that of conventional water. Such magnetic polymers are more easily adopted in certain coating applications and can further be better controlled using magnetic fields than denser, cross-linked polymers which possess much higher Prandtl numbers (~100). Commercial examples include the Aqualon™ aqueous polymer family

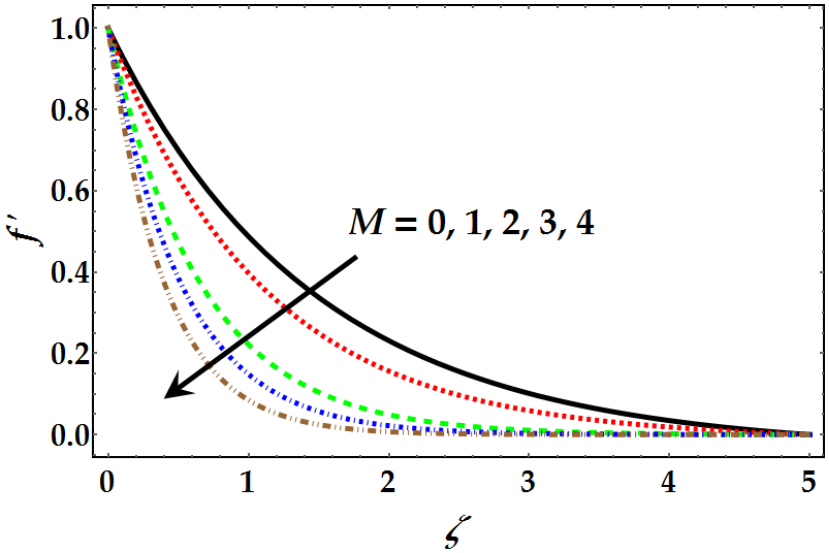

Figure 2. Velocity profile for different values of M when $P_r = 6.2, R_d = 0.5, \beta_e = 0.2, \beta_i = 0.2, B_i = 0.5, \beta = 1$.

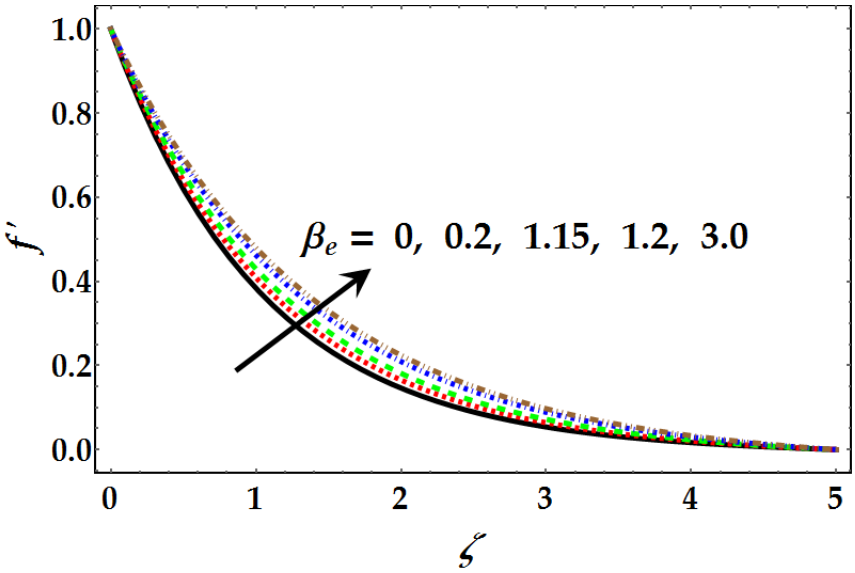

Figure 3. Velocity profile for different values of β_e when $P_r = 6.2, R_d = 0.5, M = 1, \beta_i = 0.2, B_i = 0.5, \beta = 1$.

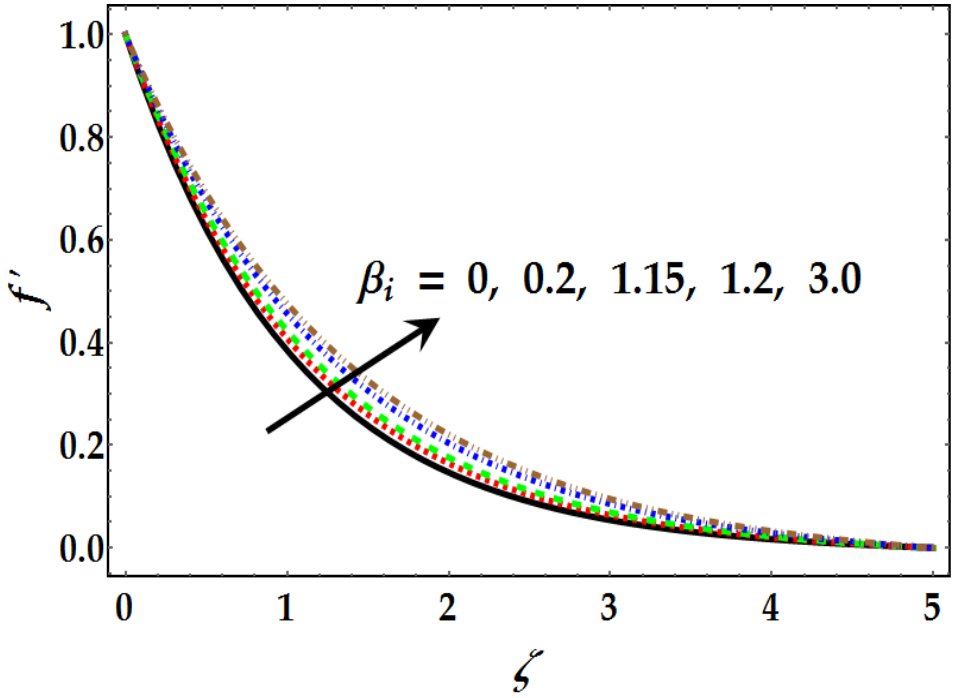

Figure 4. Velocity profile for different values of β_i when $P_r = 6.2, R_d = 0.5, M = 1, \beta_e = 0.2, B_i = 0.5, \beta = 1$.

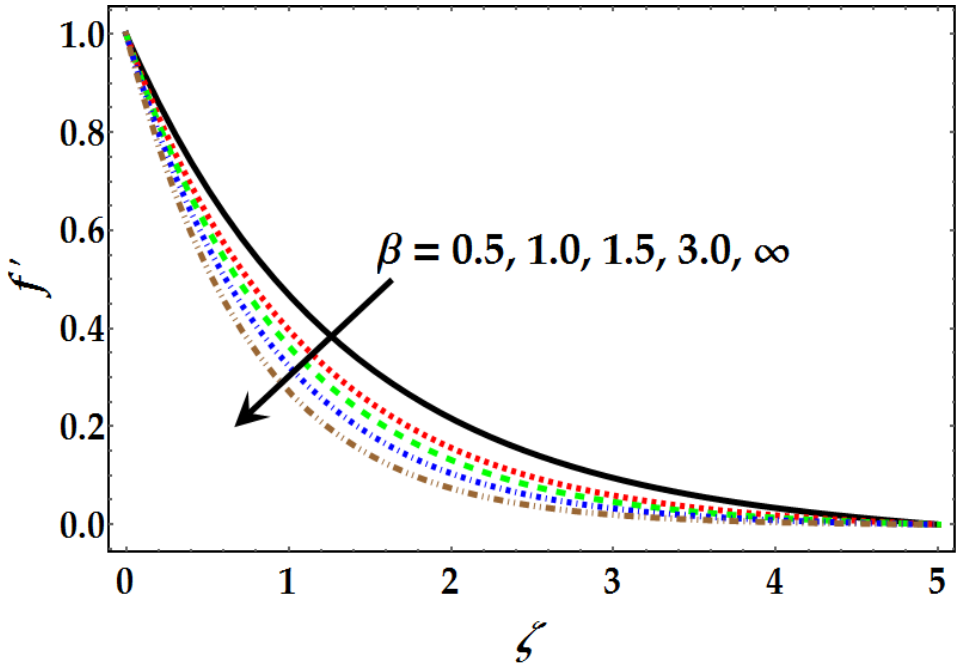

Figure 5. Velocity profile for different values of β when $P_r = 6.2, R_d = 0.5, M = 1, \beta_e = 0.2, \beta_i = 0.2, B_i = 0.5$.

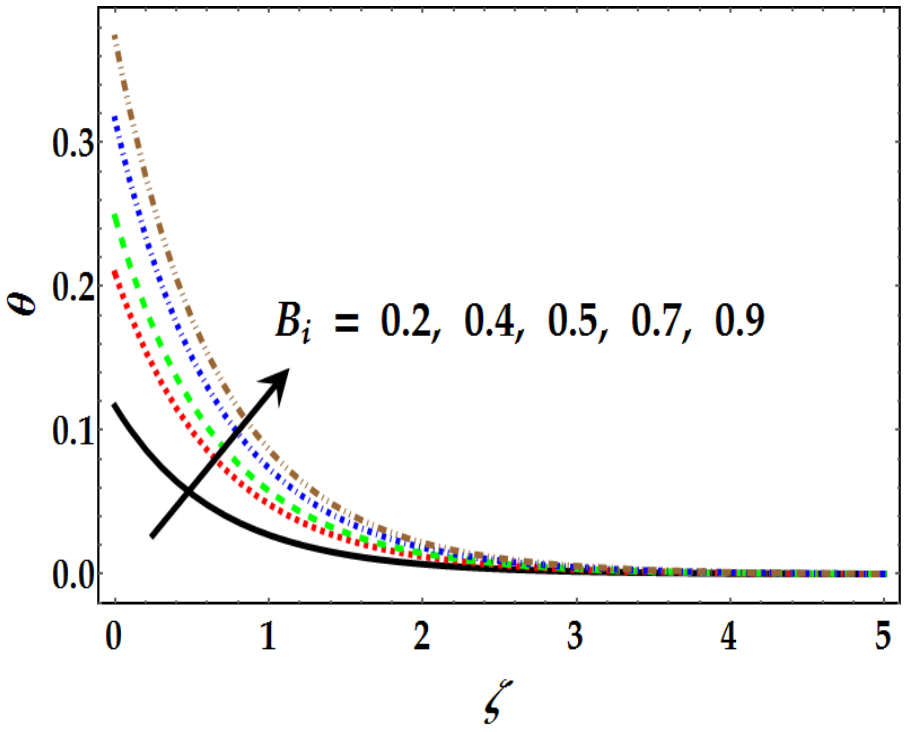

Figure 6. Temperature profile for different values of B_i when $P_r = 6.2, R_d = 0.5, M = 1, \beta_e = 0.2, \beta_i = 0.2, \beta = 1$.

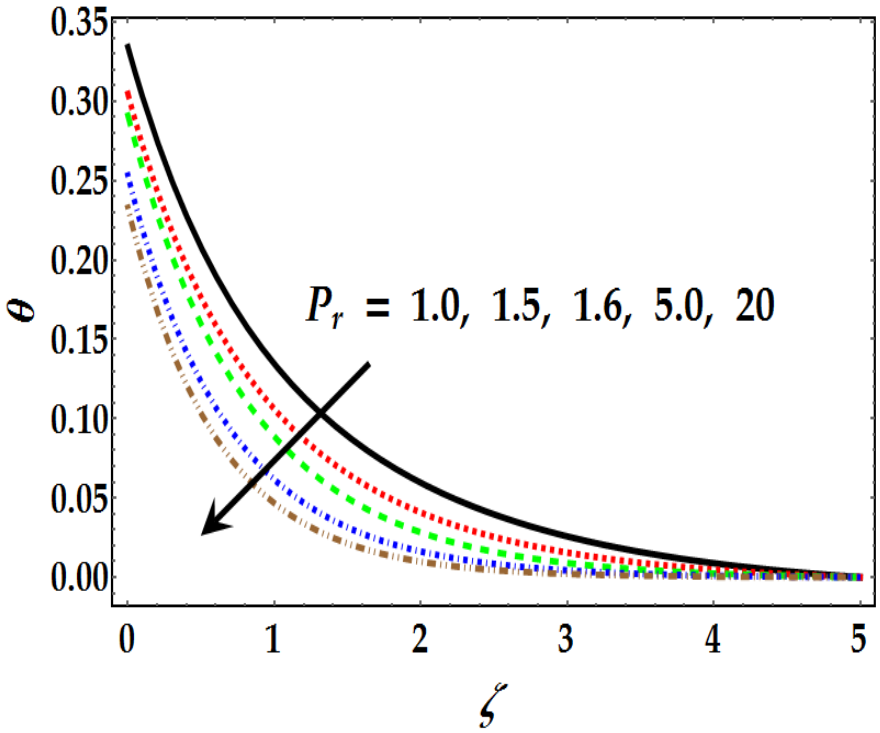

Figure 7. Temperature profile for different values of P_r when $R_d = 0.5, M = 1, \beta_e = 0.2, \beta_i = 0.2, B_i = 0.5, \beta = 1$.

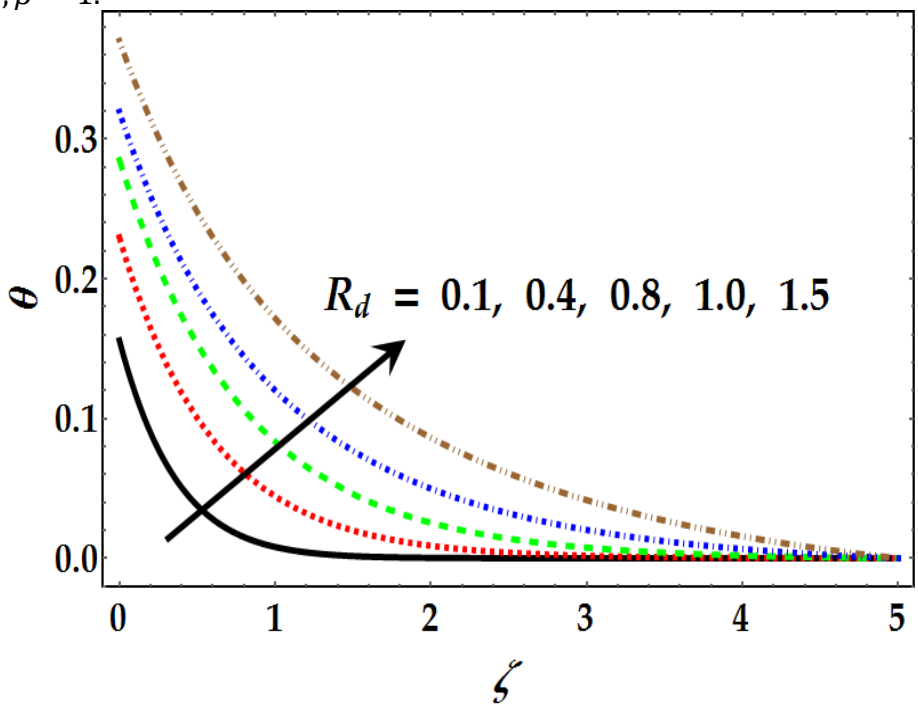

Figure 8. Temperature profile for different values of R_d when $P_r = 6.2, M = 1, \beta_e = 0.2, \beta_i = 0.2, B_i = 0.5, \beta = 1$.

Fig. (2) to Fig. (5) shows the velocity distribution with transverse coordinate for various values of

Hartmann number M, Hall parameter β_e , ion slip parameter β_i and fluid parameter β. Fig. (2) indicates that when the Hartmann number *M* increases, there is a strong deceleration induced in the boundary layer flow. The Lorentz body force in the momentum eqn. (11) is a linear term, $-\frac{M^2(1+\beta_i\beta_e)}{(1+\beta_e\beta_i)^2+\beta_e^2} f'$ and is retarding to the flow. This damps the velocity but even at maximum Hartmann number i.e. for the strongest applied magnetic field (M = 4), no flow reversal is generated. Momentum boundary layer thickness in the magnetic polymer is therefore increased with greater Hartmann number. Evidently significant flow control is achievable with appropriate selection of the magnetic field strength and furthermore a homogenous velocity distribution is achieved throughout the boundary layer. For the case M = 0, magnetic field effects are eliminated, and the polymer is electrically non-conducting and achieves a maximum flow acceleration.

We also note that in aqueous magnetic polymer dynamics, *M = 1 to 2* is a strong magnetic field range [33]. Exceeding this range may induce molecular dissociation effects, magnetic induction etc. At M = 1 the magnetic body force is of the same order as the viscous force and this is a strong magnetic field scenario for aqueous polymer processing. In other applications, this may be weak e.g. pulsed MHD power, where M ~ 4 corresponds to strong magnetic field which is required in for example seeded potassium fluid media to generate Hall currents. However, in aqueous polymer processing the threshold is much lower and Hall currents are mobilized at much lower applied magnetic fields. This is why we considered *M = 2 as the maximum strength case* and generally used M = 1 as the standard case for simulations. The present simulations have therefore used data based on real industrial studies e.g. [33].

Fig. (3) and Fig. (4) illustrate that with increasing Hall parameter β_e and ion slip parameter β_i the reverse effect is generated in the velocity distribution as observed for increasing Hartmann number. Strong flow acceleration is produced indicating that the modification in electrical conductivity associated with Hall current (cross flow) and ion slip phenomena enhances velocity magnitudes. Therefore, maximum velocity is attained with high values of these parameters and the momentum boundary layer thickness is reduced considerably. Similar observations have been reported by Pal *et al.* [26] and Shateyi and Motsa [29]. The quadratic terms in the denominator in the Lorentz body force term i.e. $(1+\beta_e\beta_i)^2+\beta_e^2$ are strongly elevated with increasing β_e and β_i values which effectively depletes the magnitude of the Lorentz force. This generates flow acceleration since there is a lower impedance due to magnetic field acting on the flow, as noted by Cramer and Pai [24] and later confirmed by Zueco *et al.* [31]. The enhancement in velocity

magnitudes with greater Hall and ion slip effect (and associated decrease in momentum boundary layer thickness) is however less dramatic than the depletion in velocity with greater Hartmann number, as also emphasized by Ramesh *et al*. [27] and Bég *et al.* [32]. There is evidently a complex inter-play between magnetic field, ion slip and Hall currents and careful selection of these parameters is required in practical materials processing operations as noted by Davidson [9].

Fig. (5) depicts the response in velocity profiles to a change in Casson viscoplastic parameter, β. With increasing β, the flow is strongly decelerated throughout the boundary layer transverse to the sheet surface. Minimum velocity is associated with the Newtonian case ($\beta \to \infty$) for which the momentum boundary layer thickness is maximized. The deceleration in the Casson flow is due to the necessity of a yield stress to be attained prior to viscous flow initiation in viscoplastic, shear-thinning polymers. The viscoplastic parameter in the momentum eqn. (11), modifies the shear term f''' in the momentum boundary layer Eqn. (11) with an inverse factor, $1/\beta$, and effectively assists momentum diffusion for small values of β. This leads to a thinning in the hydrodynamic boundary layer and associated acceleration; however, at very high values of Casson parameter (infinity is taken to be $\beta = 10^3$). the reverse effect is induced i.e. marked deceleration. Significant deviation in viscoplastic flow and Newtonian flow is observed.

Fig. (6) to Fig. (8) illustrate the temperature profiles for various values of thermal Biot number B_i, Prandtl number P_r and radiation parameter R_d. The constant wall temperature can be obtained by taking $\theta(0) = 1$ for large values Biot number B_i. It can be seen from Fig. (6) that an increment in thermal Biot number B_i creates an increment in heat transfer coefficient and this results in an enhancement in the temperature distribution. Thermal Biot number appears in the wall boundary condition in Eqn. (13) i.e. $\theta'(0) = B_i(\theta(0) - 1)$. Maximum enhancement clearly manifests at the wall (sheet surface) and progressively decays further from the wall. Attention has been confined to the *thermally-thick case* i.e. *Bi* > 0.1 for which temperature distribution is not constant throughout the fluid body (since this represents real magnetic polymers [10]). Constant temperature is only achieved for the *thermally-thin* case i.e. *Bi*<0.1. Asymptotically smooth values are achieved in the free stream indicating that a sufficiently large infinity boundary condition has been prescribed in the DTM solution. Fig. (7) illustrates the evolution in temperatures with Prandtl number P_r. It can be noticed from this figure that an increment in Prandtl number P_r causes a reduction in the temperature distribution. Polymers with lower Prandtl numbers possess higher thermal conductivities (magnetic polymers benefit from metallic doping which strongly enhances

thermal conductivity [11]). This encourages thermal conduction in the fluid and elevates temperatures. However larger Prandtl numbers imply a reduced thermal conductivity which will suppress heat diffusion in the polymer and will significantly reduce temperatures. Thermal boundary layer thickness will therefore be decreased with increasing Prandtl number. Prandtl number also expresses the ratio of momentum diffusivity to thermal diffusivity. When Prandtl number $P_r = 1$ then energy diffusion and viscous (momentum) diffusion rates are equivalent as are the momentum and thermal boundary layer thicknesses. It can be noticed from Fig. (8) that increasing radiation parameter R_d enhances the temperature profile and thermal boundary layer thickness. This parameter feature sin the augmented diffusion term in the energy conservation Eqn. (12) i.e. $\left(\frac{1}{P_r} + \frac{4}{3}R_d\right)\theta''$. $R_d = \frac{4\bar{\sigma}\tilde{T}^3}{\rho c_p \bar{k}}$, and embodies the relative contribution of *thermal radiation heat transfer* to *thermal conduction heat transfer*. For $R_d = 0$ radiative flux vanishes. As R_d increases the Casson magnetic polymer regime is progressively energized via radiation and temperatures are strongly boosted. The most dramatic impact is nearer the wall although the temperature elevation is sustained some distance from the wall. Evidently in mathematical models of high-temperature materials processing of magnetic polymers, the neglection of radiative heat transfer will significantly *under-predict* temperatures. It is important to include radiative effects albeit with simple algebraic flux models and in this regard the Rosseland model does capture the modification in temperatures quite reasonably. Similar observations have been made in Lu *et al.* [26] and Bég *et al*. [29].

5. CONCLUSIONS

In this article, stimulated by further investigating multi-physical magnetic polymer manufacturing processes, a mathematical model has been developed for viscoplastic magnetohydrodynamic flow from a stretching sheet with radiative heat transfer, Hall and Ion slip effects. The Casson model has been adopted. A convective wall thermal boundary condition has also been considered. The dimensionless momentum and energy boundary layer equations have been solved with a powerful analytical technique known as the differential transform method (DTM). Validation of solutions with the ND Solve routine in Mathematica symbolic software has been conducted. The computations have shown that:

(i)Increasing Hartmann number (magnetic field parameter) retards the flow whereas increasing Hall parameter and ion slip parameter enhance the velocity magnitudes.

(ii) Increasing thermal Biot number and radiation parameter both elevate the temperature distribution whereas increasing Prandtl number suppresses temperatures.
(iii)Increasing Casson viscoplastic parameter significantly decelerates the flow and leads to a thickening in the momentum boundary layer.
(iv) Considerable digression in results is noted between Newtonian ($infinite\ value\ of\ Casson\ parameter, \beta \to \infty$) and non-Newtonian (finite values of Casson parameter) cases indicating that rheology of electro-conductive polymers is essential for inclusion in robust mathematical models.

The differential transform method (DTM) is found to be very stable and adaptive for resolving nonlinear magnetic materials processing transport phenomena problems. Future studies will examine *double-diffusive* convection flows and other non-Newtonian (e.g. micropolar) models and will be reported soon.

Conflict of interest: The authors declare no conflict of interest.

Acknowledgements
The authors are grateful to the reviewer for his/her comments which improved the article clarity.

REFERENCES

[1] C.D. Han, *Rheology in Polymer Processing,* Academic Press, Orlando, USA (1976).

[2] Jaluria, Y., Heat and mass transfer in the extrusion of non-Newtonian materials, *Adv. Heat Transfer,* 28, 145–230 (1996).

[3] Jaluria, Y., Transport from continuously moving materials undergoing thermal processing, *Ann. Rev. Fluid Mech*., 4, pp. 187–245 (1992).

[4] Hayat T, Sajid M. Analytic solution for axisymmetric flow and heat transfer of a second-grade fluid past a stretching sheet. *Int. J. Heat. Mass Trans.*,50: 75-84 (2007).

[5] Nadeem S, Mehmood R, Akbar NS. Non-orthogonal stagnation point flow of a nano non-Newtonian fluid towards a stretching surface with heat transfer. *Int. J. Heat. Mass Trans.* 57: 679-689 (2013).

[6] Nur Amalina Latiff, Md. Jashim Uddin, O. Anwar Bég and Ahmad Izani Md. Ismail, Unsteady forced bioconvection slip flow of a micropolar nanofluid from a stretching/ shrinking sheet, *Proc. IMECHE- Part N: J. Nanoengineering and Nanosystems,* 230 (4) pp. 177–187 (2016).

[7] Hayat T, Mustafa M, Asghar S. Unsteady flow with heat and mass transfer of a third-grade fluid over a stretching surface in the presence of chemical reaction. *Nonlinear Anal-Real.*; 11: 3186-3197 (2010).

[8] O. Anwar Bég, J. Zueco and S.K. Ghosh Unsteady natural convection of a short-memory viscoelastic fluid in a non-Darcian regime: network simulation, *Chemical Engineering Communications*, 198, 172-190 (2010).

[9] P. A. Davidson, Magnetohydrodynamics in materials processing, *Ann. Rev. Fluid Mech.*, 31:273-300 (1999).

[10] G. Longo *et al.*, Morphological characterization of innovative electroconductive polymers in early stages of growth, *Surface and Coatings Technology*, 207, 286-292 (2012).

[11] J. Thévenot, Magnetic responsive polymer composite materials, *Chem. Soc. Rev.*, 42, 7099-7116 (2013).

[12] D. Gupta, L. Kumar, O. Anwar Bég and B. Singh, Finite element simulation of nonlinear magneto-micropolar stagnation point flow from a porous stretching sheet with prescribed skin friction, *Computational Thermal Sciences*, 7 (1): 1–14 (2015).

[13] M. Kumar, G. J. Reddy, N. N. Kumar and O. Anwar Bég, Computational study of unsteady couple stress magnetic nanofluid flow from a stretching sheet with Ohmic dissipation, *Proc. IMechE-Part N: J Nanoengineering, Nanomaterials and Nano-systems* (2019). (15 pages) DOI: 10.1177/2397791419843730

[14] B. Vasu, Atul Kumar Ray, O. Anwar Bég and Rama Subba Reddy Gorla, Magneto-bioconvection flow of a Casson thin film with nanoparticles over an unsteady stretching sheet: HAM and GDQ computation, *Int. J. Numerical Methods Heat Fluid Flow (2019). 33 pages. doi.org/10.1108/HFF- 02-2019-0158.*

[15] Prasad KV, Pal D, Umesh V, Rao NP. The effect of variable viscosity on MHD viscoelastic fluid flow and heat transfer over a stretching sheet. *Commun. Nonlinear. Sci. Numer. Simul.* 15: 331-344 (2010).

[16] Bergman, T.L. and Viskanta, R.: Radiation heat transfer in manufacturing and materials processing, in *Radiative Transfer-I, M.P. Menguc, Editor*, pp. 13–39, Begell House, New York (1996).

[17] M.J. Uddin, O. Anwar Bég and A.I. Ismail, Radiative-convective nanofluid flow past a stretching/shrinking sheet with slip effects, *AIAA J. Thermophysics Heat Transfer, 29, 3, 513-523 (2015).*

[18] Abo-Eldahab EM, El Gendy MS. Radiation effect on convective heat transfer in an electrically conducting fluid at a stretching surface with variable viscosity and uniform free stream. *Phys. Scripta.* 62: 321 (2000).

[19] Hayat T, Shehzad SA, Alsaedi A. Three-dimensional stretched flow of Jeffrey fluid with variable thermal conductivity and thermal radiation. *Appl. Math. Mech.* 34: 823-832 (2013).

[20] Hayat T, Shafiq A, Alsaedi A. Effect of Joule heating and thermal radiation in flow of third grade fluid over radiative surface. *Plos one.* 9: e83153 (2014).

[21] M. M. Bhatti, A. Shahid, O. Anwar Bég and A. Kadir, Numerical study of radiative Maxwell viscoelastic magnetized flow from a stretching permeable sheet with the Cattaneo–Christov heat flux model, *Neural Computing and Applications*, 30 (11) 3467–3478 (2018).

[22] Bhatti MM, Abbas T, Rashidi MM, Ali ME. Numerical simulation of entropy generation with thermal radiation on MHD Carreau nanofluid towards a shrinking sheet. *Entropy.* 18: 200 (2016).

[23] Bhatti MM, Rashidi MM. Effects of thermo-diffusion and thermal radiation on Williamson nanofluid over a porous shrinking/stretching sheet. *J. Mol. Liq.* 221: 567-573 (2016).

[24] K.C. Cramer and S. Pai, *Applied Magnetofluid Dynamics for Engineers and Applied Physicists,* MacGraw-Hill, New York, USA (1973).

[25] O. Anwar Bég, L. Sim, J. Zueco and R. Bhargava, Numerical study of magnetohydrodynamic viscous plasma flow in rotating porous media with Hall currents and inclined magnetic field influence, *Comm. Nonlinear Science and Numerical Simulation*, 15, 345-359 (2010).

[26] D. Pal *et al.* Effects of Hall current and chemical reaction on oscillatory mixed convection-radiation of a micropolar fluid in a rotating system, *Chem. Eng. Comm.*, 199, 943-965 (2012).

[27] K. Ramesh, D. Tripathi, O. Anwar Bég, A. Kadir, Slip and Hall current effects on viscoelastic fluid-particle suspension flow in a peristaltic hydromagnetic blood micropump, *Iranian Journal of Science and Technology, Transactions of Mechanical Engineering (2018). doi.org/10.1007/s40997-018-0230-5 (18 pages)*

[28] H. Attia, Analytical solution for flow of a dusty fluid in a circular pipe with Hall and ion slip effects, *Chem. Eng. Comm.*, 194, 1287-1296 (2007).

[29] S. Shateyi and S.S. Motsa, Boundary layer flow and double diffusion over an unsteady stretching surface with Hall effect, *Chem. Eng. Comm.*, 198, 1545-1565 (2011).

[30] R. Choudhury and P. Dhar, Ion slip effect on viscoelastic fluid flow past an impulsively started infinite vertical plate embedded in a porous medium with chemical reaction, *Int Sch Res Notices*. 2014: 481308 (2014).

[31] J. Zueco, O. Anwar Bég and L.M. Lopez-Ochoa, Non-linear transient hydromagnetic partially ionised dissipative Couette flow in a non-Darcian porous medium channel with Hall, ionslip and Joule heating effects, *Progress in Computational Fluid Dynamics,* 11, 2, 116-129 (2011).

[32] O. Anwar Bég, S. Abdul Gaffar, V. Ramachandra Prasad and M.J. Uddin, Computational solutions for non-isothermal, nonlinear magnetoconvection in porous media with Hall/ionslip currents and Ohmic dissipation, *Engineering Science and Technology-an International Journal*, 19, 377-394 (2016).

[33] H. J Schneider-Muntau and H. Wada (Eds)., Materials Processing in Magnetic Fields, *Proceedings of the International Workshop on Materials Analysis and Processing in Magnetic Fields, Tallahassee, Florida, USA, 17 – 19 March* (2004)

[34] Abolbashari MH, Freidoonimehr N, Nazari F, Rashidi MM. Analytical modeling of entropy generation for Casson nano-fluid flow induced by a stretching surface. *Adv. Pow. Technol.* 26: 542-552 (2015).

[35] V.R. Prasad, A. SubbaRao, N. Bhaskar Reddy, B. Vasu, O. Anwar Bég, Modelling laminar transport phenomena in a Casson rheological fluid from a horizontal circular cylinder with partial slip, *Proc IMechE- Part E: J. Process Mechanical Engineering, 227 (4) 309-326 (2013).*

[36] N. S. Akbar, D. Tripathi, O. Anwar Bég, Z. H. Khan, MHD dissipative flow and heat transfer of Casson fluids due to metachronal wave propulsion of beating cilia with thermal and velocity slip effects under an oblique magnetic field, *Acta Astronautica, 128, 1-12 (2016).*

[37] J.K. Zhou, J.K. *Differential Transformation and Its Applications for Electrical Circuits.* Huazhong University Press, Wuhan, China (1986).

[38] D. Tripathi, O. Anwar Bég, P.K. Gupta, G. Radhakrishnamacharya and J. Mazumdar, DTM simulation of peristaltic viscoelastic biofluid flow in asymmetric porous media: a digestive transport model, *Journal of Bionic Engineering,* 12 (4) 1-13 (2015).

[39] M.M. Rashidi, N. Kavyani, O. Anwar Bég and R.S.R. Gorla, Transient magnetohydrodynamic film flow, heat transfer and entropy generation from a spinning disk system: DTM-Padé semi-numerical simulation, *Int. J. Energy & Technology* 5 (18), 1–14 (2013).

[40] M. Kumar, G. J. Reddy, N. N. Kumar and O. Anwar Bég, Application of differential transform method to unsteady free convective heat transfer of a couple stress fluid over a stretching sheet, *Heat Transfer - Asian Research (Japan) (2018). DOI: 10.1002/htj.21396 (19 pages)*

[41] O. Anwar Bég, M.M. Rashidi, A. Aziz and M. Keimanesh, Differential transform study of hypersonic laminar boundary layer flow and heat transfer over slender axisymmetric bodies of revolution, *Int. J. Applied Mathematics and Mechanics,* (6): 83 – 108 (2012).

[42] Lu, D. *et al*. On three-dimensional MHD Oldroyd-B fluid flow with nonlinear thermal radiation and homogeneous–heterogeneous reaction. *J. Brazilian Soc. Mech. Sci. Eng.* 40(8), 387 (2018).

[43] Gorla, R.S.R. and Sidawi, I., 1994. Free convection on a vertical stretching surface with suction and blowing. *Applied Scientific Research*, 52(3), pp.247-257.